Journal of Oral Rehabilitation 2006 **33**; 889–897

Biological responses of anodized titanium implants under different current voltages

J. W. CHOI, S. J. HEO, J. Y. KOAK, S. K. KIM, Y. J. LIM, S. H. KIM & J. B. LEE *Department of Prosthodontics and Dental Research Institute, College of Dentistry, Seoul National University, Korea*

SUMMARY The oxide layer of a titanium surface is very stable, and seems to result in excellent biocompatibility and successful osseointegration. The purpose of this study was to investigate the effects of high anodic oxidation voltages on the surface characteristics of titanium implants and the biologic response of rabbit tibiae. Bone tissue responses were evaluated by removal torque tests and histomorphometric analysis. Screw-shaped implants with microthreads were made of commercially pure titanium (Grade II). We prepared anodized implants under 300 V (group I), 400 V (group II), 500 V (group III) and 550 V (group IV). The surface characteristics of specimens were inspected according to three categories: surface morphology, surface roughness and oxide layer thickness. The screw-shaped implants were installed in rabbit tibiae. The removal torque values were measured and histomorphometric analysis was done after 1- and 3-month healing periods. Data indicate that as anodic oxidation voltage increased above 300 V, oxide layer thickness increased rapidly and pore size also increased. The roughness values of the implants increased with voltage up to 500 V, but decreased at 550 V. In the removal torque test, group III showed higher values than groups I and II at a statistically significant level ($P < 0{\cdot}05$) after a 1-month healing period. In histomorphometric analysis, groups III and IV, after a 3-month healing period, showed greater bone to implant contact ratios for the total implant surface than did group I ($P < 0{\cdot}05$).

KEYWORDS: anodic oxidation, voltage, histomorphometry, removal torque, titanium implant

Accepted for publication 28 June 2006

Introduction

The importance of implant surface properties for successful osseointegration was first pointed out by Albrektsson *et al.* (1). However, a number of questions have followed regarding the important role of the surface properties of titanium implants 'during dynamic build-up' of the osseointegration process (2, 3). Interest in the surface oxide properties of titanium implants has increased with the development of methods to characterize such surfaces. Moreover, the possibility of the surface modification of titanium implants to improve tissue responses is an outstanding feature in metal implantology researches.

In the air at room temperature, the surface of titanium is covered spontaneously by an oxide layer 1·5–10-nm thickness (4). It was determined that the oxide layer has a low level of electronic conductivity (5), great thermodynamic stability (6) and low ion-formation tendency in aqueous environments (7). These properties of the titanium oxide layer can be the reasons for the excellent biocompatibility of titanium implants (8). Moreover, in the study of retrieved implants from patients, the successfully osseointegrated implants showed an increase in oxide thickness up to 200 nm (9). In contrast, failed implants showed no changes in oxide thickness (10). Oxide thickness can be increased by heat treatment

doi: 10.1111/j.1365-2842.2006.01669.x

(thermal oxidation). In an earlier study, Al_2O_3-blasted and thermally oxidized titanium implants showed a better biologic response than implants that were only blasted (11).

Recently, an electrochemical procedure for modifying the Ti surface was proposed. When a positive voltage is applied to a Ti specimen immersed in an electrolyte, anodic oxidation of Ti occurs to form a TiO_2 layer on the surface. When the applied voltage is increased to a certain point, a micro-arc occurs as a result of the dielectric breakdown of the TiO_2 layer. At that moment, the Ti ions in the implant and the OH ions in the electrolyte move in opposite directions very quickly to form TiO_2 again. This process is generally referred to as micro-arc oxidation (MAO) or plasma electrolysis (12, 13). The newly formed TiO_2 layer is both porous and firmly adhered to the substrate, which is beneficial for the biological performance of the implants. Recent studies on the biological response of Ti implants demonstrated that the MAO process constitutes one of the best methods for modifying the implant surface (14, 15). However, further research is necessary for the complete characterization of the oxide layer and also for the identification of the optimum conditions for the MAO process. Knowledge is still lacking about the role of surface oxide thickness during the dynamic build-up of an osseointegration process (16).

In this study, we formed TiO_2 layers with different thicknesses and roughness on the Ti surface by controlling the applied voltage used in the MAO process. In an earlier study, implants were anodized under 190–270 V, and the implants anodized under 270 V showed better biologic responses (17). Thus, in this study, we inspected relatively high voltages. The roughness, thickness and morphology of the oxide layer were monitored with respect to the applied voltage. The biological properties of the layers were evaluated by the removal torque test and histomorphometric analysis of implants inserted in rabbit tibiae after 1- and 3-month healing periods. The purpose of this study was to investigate how surface roughness and oxide layer thickness influenced bony response in anodized implants.

Materials and methods

Implant preparation: design and surface oxide

A total of 152 square screw-shaped implants, each of which had a pitch-height of 0·9 mm, an outer diameter of 4·3 mm, a length of 8·0 mm and were external hexa-headed, were turned from 5-mm rods of commercially pure titanium (ASTM Grade II). All surface oxides used in the present study were prepared with the use of a direct current (DC) power supply in electrolyte solution. The implant samples were divided into four groups according to the anodic forming voltage, as follows:

Group I implants ($n = 38$): electrochemically prepared surface oxides up to forming voltage of 300 V.

Group II implants ($n = 38$): electrochemically prepared surface oxides up to forming voltage of 400 V.

Group III implants ($n = 38$): electrochemically prepared surface oxides up to forming voltage of 500 V.

Group IV implants ($n = 38$): electrochemically prepared surface oxides up to forming voltage of 550 V.

Micro-arc oxidation

Micro-arc oxidation of the specimens was carried out in an aqueous electrolyte by applying a pulsed DC field to the specimens. The frequency was 660 Hz. The electrolyte was prepared by dissolving 0·15 M calcium acetate monohydrate Ca(CH3COO)2·H2O and 0·02 M calcium glycerophosphate (CaC3H7O6P) in de-ionized water. A high range of DC fields (300, 400, 500 and 550 V) were applied to the specimens, with each treatment lasting 3 min. All of the MAO processing was carried out in a water-cooled bath made of stainless steel, and a stainless steel plate (100 × 60 × 1 mm) was used as the counter electrode.

Characterization of oxide layer

The microstructures of the specimens were evaluated by scanning electron microscopy (s.e.m., JSM-5600*). Images taken by s.e.m. were analysed by an image analysis program† to measure the pore sizes of the specimens. The thickness of the oxidized layer was examined using a cross-sectional s.e.m. at an acceleration voltage of 300 kV. The surface roughness was measured by means of an optical interferometer (Accura 2000®‡). The average roughness (R_a) was used to characterize the roughness of the specimens. R_a indicates an arithmetic average

*JEOL, Tokyo, Japan.
†Image Access, Bildanalyssystem AB, Sweden.
‡Intekplus Co., Seoul, Korea.

[$R_a = (z1 + z2 + z3 + \ldots + zN)/n$], and the cutoff length was 0·25 mm.

Animals and surgical technique

Thirty mature (average age, 10 months old; weight, 3–3·5 kg) New Zealand white rabbits of both sexes were included in this study. During surgery, the animals were anaesthetized with i.m. injections of ketamine[§] (10 mg kg^{-1}) and Rompune[¶] (0·15 mg kg^{-1}). Prior to surgery, the shaved skin was carefully washed with a mixture of iodine and 70% ethanol. Local anesthesia with 1·0 ml of 5% lidocaine§ (1:100 000 epinephrine) was administered at the tuburositas tibiae part of the bone where the incision was planned, under aseptic conditions. The skin and fascial layers were opened and closed separately. The periosteal layer was gently pulled away from the surgical area and was not re-sutured. During all surgical drilling sequences, low rotary drill speeds, not exceeding 1000 rpm, and profuse saline cooling were used.

Each rabbit had two implants inserted in each tibia; these penetrated one cortical layer only. The implants were inserted in a predetermined-randomized design that enabled multiple comparisons. The animals were kept in separate cages, and immediately after surgery, they were allowed to be fully weight-bearing. Rabbits were sacrificed by i.v. injections of PentobarbitalumA[§] at the scheduled time.

Removal torque measurements

Sixteen rabbits were sacrificed for removal torque tests, eight rabbits after 1 month and eight rabbits after 3 months from the first surgery. The removal torque values of 64 implants were measured. Fixture mounts were connected and were placed in the torque measurement device**. Then, removal torque values were measured. Histomorphometric measurements provide rational information about healing responses, but give us only two-dimensional data. Removal torque measurements can be regarded as three-dimensional tests that roughly reflect the interfacial shear strength between bone tissue and the implant.

Preparation of specimens and histomorphometric analysis

Fourteen rabbits were sacrificed for histomorphometric analysis, seven rabbits after 1 month and seven rabbits after 3 months. Fifty-six implants were prepared for histomorphometric analysis. The implants and surrounding bone were fixed in neutral buffered formalin, dehydrated in 70%, 90%, 95% and 100% alcohol, and embedded in a light-curing resin[††] (Technovit 7200 VLC). The cutting and grinding were performed with a sawing machine and grinding equipment[‡‡]. The sections were approximately 10-μm thick, and were stained with toluidine blue. The histomorphometric analysis was performed with the help of an Olympus BX microscope[§§] connected to a computer. The software used was KAPPA IMAGE ANALYSIS[¶¶]. All measurements were calculated with a 4× magnification objective and with eyepieces of 25× magnification. The percentages of bone to implant contact (BIC) in the three best consecutive threads and of the total implant surface were calculated. The percentage of bone inside the three best consecutive threads was calculated. A higher magnification objective and zoom were used to help decide whether or not the bone was in contact with the implant surface. The BIC ratio of the total implant surface was calculated as (total contact surface length/total implant surface length).

Statistic analysis

SPSS*** 12·0 for Windows was used to carry out statistical analysis. One-way analysis of variance (ANOVA) was used for statistical analysis of the topographical data, removal torque measurement data and histomorphometric analysis data.

Results

Characteristics of oxide layer

The surface morphologies of titanium implants after MAO using different current voltage conditions are shown in Fig. 1. At the voltage of 300 V, the layer

[§]Yu-han Co., Seoul, Korea.
[¶]Bayer Korea Co., Seoul, Korea.
**Shinsung Co., Seoul, Korea.

[††]Kulzer, Wehrheim, Germany.
[‡‡]Exakt Apparatebau, Norderstedt, Germany.
[§§]Olympus Co., Tokyo, Japan.
[¶¶]KAPPA Opto-electronics Gmbh, Gleichen, Germany.
***SPSS, Chicago, IL, USA.

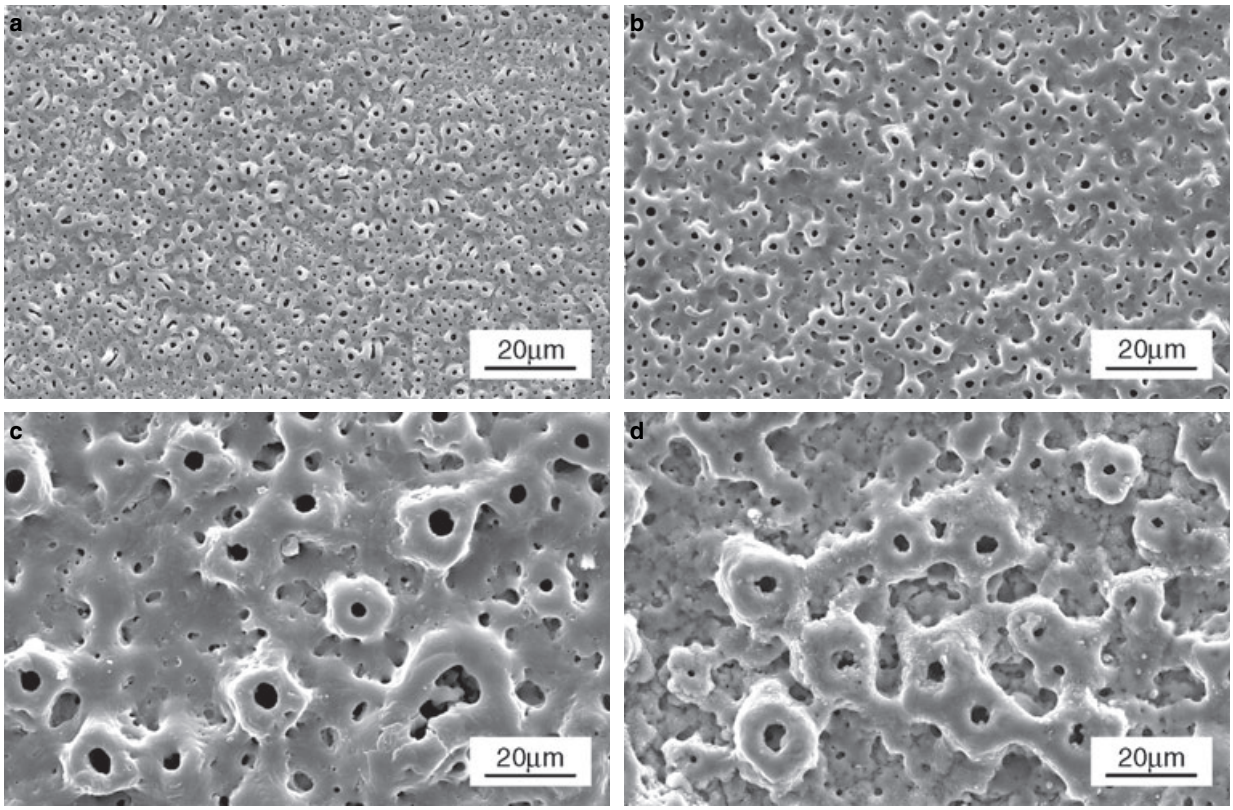

Fig. 1. Scanning electron microscope views of surface morphologies of titanium surfaces treated with micro-arc oxidation at different voltages. (a) 300 V, (b) 400 V, (c) 500 V and (d) 550 V.

became uniformly porous (Fig. 1a). The resulting layer was actually composed of small craters with holes at the centre. When the voltage was increased to 400 V, the size of these craters became so large that they were connected together, as shown in Fig. 1b, and the presence of tiny cracks was observed. When the voltage attained 500 V, the size of the holes, as well as that of the craters, became much larger (Fig. 1c), and this trend continued as the applied voltage was further increased up to 550 V (Fig. 1d). Above 300 V, the thickness of the layer increased with increasing voltage. The thickness of the layer was measured as a function of the applied voltage (Fig. 2). As expected, the thickness was almost linearly dependent on the voltage. Surface roughness was measured with an optical interferometer. The roughness of the oxide layer was characterized on the implant itself by the R_a. As the applied voltage increased, R_a values increased rapidly, as shown in Fig. 3. The surface roughnesses of group III ($R_a = 5{\cdot}2$ μm) and group IV ($R_a = 3{\cdot}8$ μm) were significantly higher than group I ($R_a = 0{\cdot}8$ μm) and group II ($R_a = 1{\cdot}7$ μm) (group III > group I at $P = 0{\cdot}005$, group III > group II at $P = 0{\cdot}016$, group IV > group I at $P = 0{\cdot}010$, group IV > group II at $P = 0{\cdot}038$). Roughness decreased above 500 V. In brief, surface morphology was a porous structure in groups I through IV. In group I, the pore size was 1-μm diameter, while the pore size increased according to the forming voltage

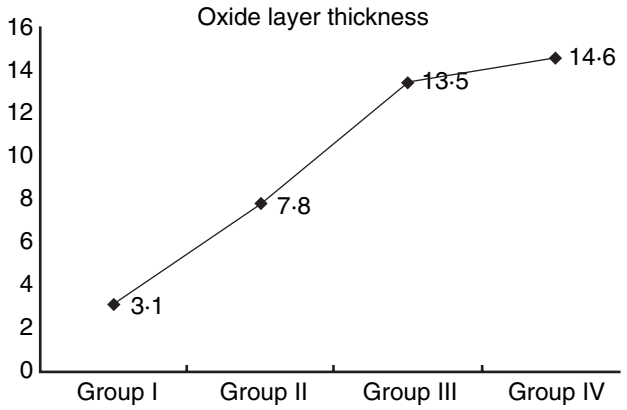

Fig. 2. Thickness of oxide layer as a function of the applied voltage (μm).

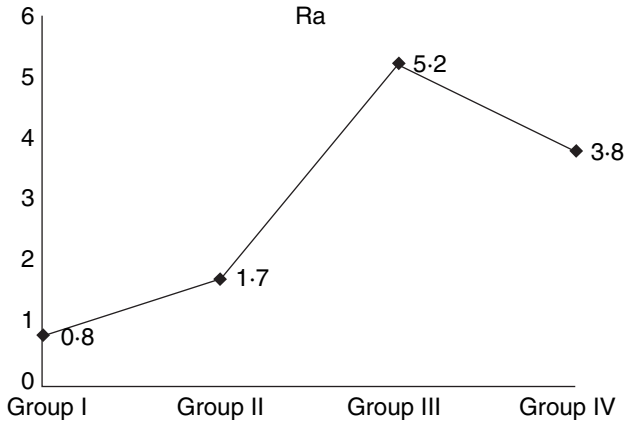

Fig. 3. Surface roughness (R_a, μm) of the titanium implants. R_a: arithmetic mean of the absolute values of the surfaces.

that was applied, reaching 2 μm in group II and 3 μm in groups III and IV. Oxide thickness increased rapidly with oxidation voltage from 3·1 μm (group I) to 14·6 μm (group IV). Surface roughness also increased with oxidation voltage from 0·8 μm (group I) to 5·2 μm (group III). The various oxide properties in this study are summarized in Table 1.

Removal torque results

The removal torque values of 16 rabbits after 1 and 3 months were summarized in Table 2. After 1 month, the removal torques of group III (48·4 Ncm) and group IV (45·2 Ncm) were bigger than those of group I (39·1 Ncm) and group II (38·7 Ncm). The removal torque of group III was significantly larger than those of groups I and II (group III > group I at $P = 0{\cdot}041$, group III > group II at $P = 0{\cdot}044$). After 3 months, the data showed no significant differences.

Histomorphometric results

Qualitative evaluation on 10-μm thick toluidine blue-stained cut and ground sections. In general, the gross observations of the tissue structures between groups were rather similar. Newly formed bone tissue could be observed in the periosteal and in the endosteal regions, while the tissue structures in the old cortical region were remodelled, as indicated by darker stained younger bone and a pale staining of the original cortex (Fig. 4a). Focusing on the interface region, a very thin black line could occasionally be observed, separating the bulk implant from the tissue in all groups. Sometimes, this line was delaminated from the bulk implant and attached to the tissue. This layer was the oxide layer, and could be separated from the titanium bulk trough a ground sectioning procedure (Fig. 4b). Apical in the area of the implant facing the marrow cavity, solitary areas or peninsulas of newly formed bone tissue were observed inside the threads. The bone marrow structure was observed close to the implant surface (Fig. 4c).

Quantitative histomorphometrical evaluation of toluidine blue-stained cut and ground sections. The BIC ratio of total implant surface data is summarized in Table 3 (Fig. 5). After a 1-month healing period, data showed no significant difference. However, after 3 months, BIC increased as oxidation voltage increased. The BICs of group III (43·3%) and group IV (43·6%) were significantly bigger than that of group I (33·0%) (group III > group I at $P = 0{\cdot}042$, group IV > group I at $P = 0{\cdot}045$).

Three best consecutive threads were chosen from each specimen and measured for BIC and bone area. Data are summarized in Tables 4 and 5. BIC values were very high, above 60%, even after a 1-month healing period, and bone area values were above 70%. However, the data showed no significant differences between groups.

Discussion

The microstructural change of the oxide layer was found to be closely related to the voltage used for the MAO treatment. Increasing the voltage resulted in

Table 1. Summary of oxide growth parameters and surface characteristics of the four different types of c.p. titanium implants

Oxide layer characteristics	Group I	Group II	Group III	Group IV
Anodic forming voltage	300 V	400 V	500 V	550 V
Oxide thickness	3·1 μm	7·8 μm	13·5 μm	14·6 μm
Morphology	porous	porous	porous	porous
Pore size	1 μm	2 μm	3 μm	3–3·5 μm
Roughness (R_a)	0·8 μm	1·7 μm	5·2 μm	3·8 μm

	Group I	Group II	Group III	Group IV
1-month healing period	37·3 ± 8·2	36·4 ± 3·8	49·6 ± 9·9	46·4 ± 8·6
3-month healing period	42·8 ± 4·1	44·6 ± 7·9	44·6 ± 7·7	43·6 ± 6·5

Table 2. Removal torque values (Ncm) of anodized implants after 1- and 3-month healing periods (mean ± s.d.)

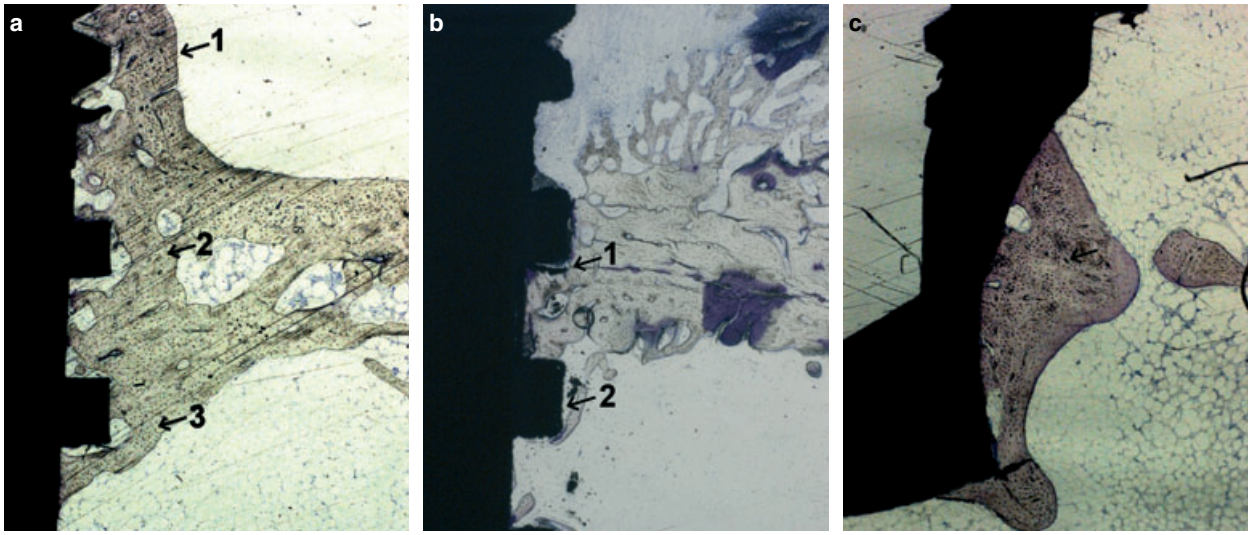

Fig. 4. Qualitative analysis of 10-μm thick toluidine blue-stained cut and ground section. (a) Periosteal and endosteal bone formation: 1: periosteal new bone formation, 2: old cortical bone, 3: endosteal new bone formation; (b) the delaminated dark line was the separated oxide layer; 1: separated oxide layer, 2: thick oxide layer; (c) solitary area of new bone formation.

	Group I	Group II	Group III	Group IV
1-month healing period	26·2 ± 4·1	20·9 ± 3·3	23·8 ± 4·7	21·1 ± 2·7
3-month healing period	30·9 ± 7·7	35·0 ± 7·4	45·9 ± 9·6	46·2 ± 8·5

Table 3. Bone to implant contact ratio of total implant surface (mean ± s.d.)

increases in both the roughness and pore size, as well as in the thickness of the oxide layer (Figs 1 and 2). These microstructural evolutions are attributed to the dielectric breakdown of the oxide layers (20). During the MAO process, as the TiO_2 layer becomes thicker, micro-arc discharges occur on the local area of the substrate, breaking down the surface dielectric layer to form micro pores. As the oxide layer becomes thicker, the resistance of the oxide layer increases, and a higher potential energy is required to break down the dielectric layer. As a result of this series of reactions, the pore size and the roughness of the oxide layer increase rapidly. The existence of titanium oxide on the titanium surface has been reported to improve bone formation (21, 22). An increase in surface roughness has been also known to enhance the mechanical interlocking between the implant and the bones (23). In this experiment, the removal torque of the MAO-treated titanium implants under 500 V (group III) was higher than that of other groups, and so was the roughness. This enhancement was attributable to the increase in surface roughness.

A rougher surface can engage more bone chips during surgery. These bone chips can be a possible reason for the histomorphometric result observed. In this study, all groups had thick oxide layers (>3 μm), and the BIC and bone area of the three best consecutive threads showed good bony response (Tables 4 and 5). The BICs of the three best consecutive threads showed no difference between groups, but interestingly, the BICs for the total implant surfaces of groups III and IV were significantly larger than for group I after a 3-month healing period (Table 3). This means more periosteal and endosteal bone formation in groups III and IV, and roughness could be the reason for this phenomenon (Fig. 5). Groups III and IV had more rough surface than groups I and II (Fig. 3). Bone chips can induce more endosteal bone formation.

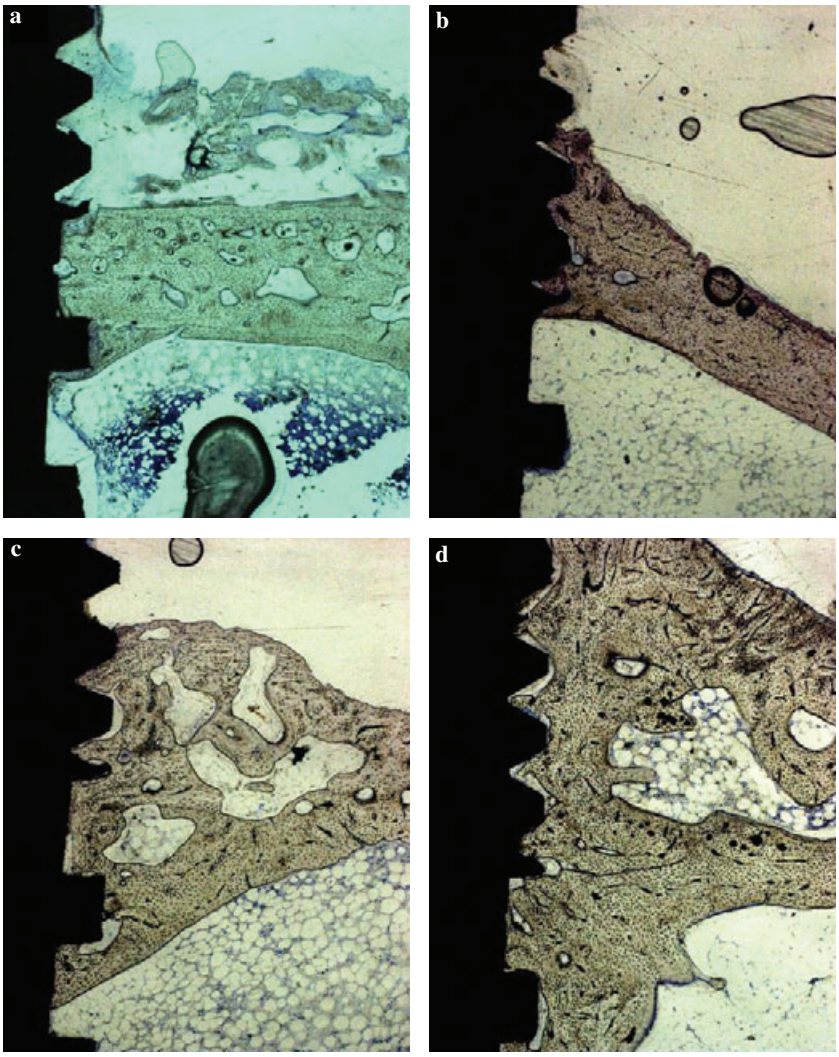

Fig. 5. Light microscopic views of anodized implants after 3 months. (a) group I, (b) group II, (c) group III and (d) group IV. In all groups, good bone-to-implant contacts were observed in the threads. (c) and (d) showed more new bone formation.

Table 4. Bone to implant contact ratio in the three best consecutive threads (mean ± s.d.)

	Group I	Group II	Group III	Group IV
1-month healing period	68·3 ± 11·3	66·9 ± 17·2	72·4 ± 16·7	72·2 ± 10·5
3-month healing period	70·4 ± 13·1	70·2 ± 16·4	68·2 ± 12·5	74·6 ± 10·6

Table 5. The percentage of bone inside the three best consecutive threads (mean ± s.d.)

	Group I	Group II	Group III	Group IV
1-month healing period	75·1 ± 15·1	74·2 ± 14·4	80·8 ± 8·8	84·9 ± 6·6
3-month healing period	82·0 ± 7·3	77·8 ± 11·0	76·9 ± 7·8	81·6 ± 10·4

However, in this study, roughness decreased above 500 V (Fig. 3). An extremely high oxidation voltage could electropolish the titanium surface, and this phenomenon happened on the group IV implants. In an earlier study, increasing the surface oxide thickness of titanium implants from 1 to 3 μm resulted in the simultaneous increase of the bone response (17). As anodic oxidation voltage increased, the oxide layer grew thicker, from 1·27 μm (190-V group) to 2·89 μm (270-V group), the pore size increased from 0·24 to 0·79 μm, and the surface roughness grew from 0·54 to 0·88 μm. Also, the removal torque of the 270-V group was higher than

that of the lower voltage groups ($P < 0{\cdot}05$). In this study, the oxide layer thickness increased from 3 to 14·6 μm, but the BIC did not increase. Oxide layers thicker than 3 μm did not produce simultaneous increases in the bony response. The morphological appearance at higher voltages demonstrated a 'molten appearance' with more extensive pores and craters and increased pore size. The extensive breakdown of the anode oxide film may also result in a network of pore channels or connected channel branches through the oxide section of increased thickness. However, this may result in a degradation of the mechanical properties necessary for biological applications of the anodic oxide film. As a matter of fact, a much thicker oxide layer prepared under high voltage may show poor mechanical properties; light microscopic observations of cut and ground sections of implants in animals revealed that such a thick oxide film delaminated (Fig. 4b), and oxide particles were internalized in the inflammatory cells, such as multinucleated giant cells. This could be another reason for the trends seen in the removal torque data. Although oxide layer thickness increased with anodic oxidation voltage, group IV (anodized under 550 V) showed a lower removal torque than group III (anodized under 500 V).

In this study, the BICs of three best consecutive threads were quite high, and did not increase through the healing period. In an earlier study of thermal oxidation (11), the BIC was 33·3% after 1 month of healing and 58·2% after 3 months of healing. The possible reasons for these results are (i) good tissue response of implants anodized above 300 V and (ii) BIC may not increase above 80% without functional stimulation. Generally, in rabbit tibiae, a larger amount of bone is observed in the threads in the old cortical region than in the threads in the marrow cavity (24). This could be one reason that the BIC of the total implant surface was relatively low when compared with that of the three best consecutive threads.

For the removal torque test, an electronic device incorporating a strain gauge transducer enables the controlled torque analysis of the peak loosening torque (18). However, a hand-controlled device may introduce the operator error, so in this study, a conventional device incorporating gravity was used. The removal torque reflects a three-dimensional measurement of the shear strength, while the histomorphometry is performed in one dimension only. However, in this study, the implants had a cutting edge for self-tapping, and sometimes cortical bone grew to this cutting edge. The removal torque value could be very high in this situation (19). Thus, the operator paid much attention to prohibit the bicortical fixation. For histomorphometric analysis, the technique of producing undecalcified cut and ground sections with implants *in situ* and of the thickness of a bone cell (10–15 μm) has been used in our laboratory. One major drawback was that this procedure was time-consuming and did not permit serial sectioning. The standardization of cutting directions and sample thickness was crucial. At least one, and sometimes two, sections were prepared from each implant. Routine histological staining with toluidine blue was performed on the most central section. In order to standardize the analysis, the most central section was always chosen for histomorphometrical quantifications. All measurements were always done by the same person.

In summary, as the anodic oxidation voltage increased above 300 V, the surface oxide layer thickness increased rapidly, and both pore size and surface roughness increased. These changes resulted in good biologic responses in rabbit tibiae. Specifically, a higher roughness can introduce more endosteal and periosteal bone formation. However, an oxide layer thicker than 3 μm did not introduce better bony response. Furthermore, in the removal torque data, group III showed better results, although group IV had a thicker oxide layer. The mechanical strength of the anodic film evidently depends on voltage in this experimental model.

Acknowledgments

This study was supported by a grant from the Korean Health 21 R&D project, Ministry of Health & Welfare, Republic of Korea (02-PJ3-PG6-EV11-0002).

References

1. Albrektsson T, Branemark PI, Hansson HA, Kasemo B, Larsson K. The interface zone of inorganic implant *in vivo*; Titanium implants in bone. Ann Biomed Eng. 1983;11:1–27.
2. Larsson C, Thomsen P, Lausmaa J, Rodahl M, Kasemo B, Eriksson LE. Bone response to surface-modified titanium implants: studies on electropolished implants with different oxide thickness and morphology. Biomaterials 1994;15:1062–1074.
3. Chun HJ, Park DN, Han CH, Heo SJ, Heo MS, Koak JY. Stress distributions in maxillary bone surrounding overdenture with different overdenture attachments. J Oral Rehabil. 2005;32:193–205.
4. Kasemo B, Lausmaa J. Aspect of surface physics on titanium implants. Swed Dent J. 1983;28(Suppl.):19–36.

5. Zitter H, Plenk HJ. The electrochemical behavior of metallic implant materials as indicator of their biocompatibility. J Biomed Mater Res 1987;21:881–896.
6. Solar RJ, Pollack SR, Korostoff E. *In vitro* corrosion testing of titanium surgical implant alloys: an approach to understanding titanium release from implants. J Biomed Mater Res 1979;13:217–250.
7. Tengvall P, Lindstrom I. Physico-chemical considerations of titanium as a biomaterial. Clin Mater. 1992;9:115–134.
8. Sul YT, Johansson CB, Jeong YS, Albrektsson T. The electrochemical oxide growth behavior on titanium in acid and alkaline electrolytes. Med Eng Phys. 2001;23:329–346.
9. Sundgren JE, Bodo P, Lundstrom I. Auger electron spectroscopic studies of the interface between human tissue and implants of titanium and stainless. J Colloid Interface Sci. 1986;110:9–20.
10. Esposito M, Lausmaa J, Hirsch JM, Thomsen P. Surface analysis of failed oral titanium implants. J Biomed Mater Res. 1999;48:559–568.
11. Kim YH, Koak JY, Chang IT, Wenneberg A, Heo SJ. A histomorphometric analysis of the effects of various surface treatment methods on osseointegration. Int J Oral Maxillofac Implants. 2003;18:349–356.
12. Yerokhin AL, Nie X, Leyland A, Matthews A, Dowey SJ. Plasma electrolysis for surface engineering. Surf Coating Tech. 1999;122:73–93.
13. Ishizawa H, Ogino M. Formation and characterization of anodic titanium oxide films containing Ca and P. J Biomed Mater Res. 1995;29:65–72.
14. Schreckenbach JP, Marx G. Characterization of anodic spark-converted titanium surface for biomedical application. J Mater Sci Mater Med. 1999;10:453–457.
15. Sul YT. The significance of the surface properties of oxidized titanium to the bone response: special emphasis on potential biochemical bonding of oxidized titanium implant. Biomaterials. 2003;24:3893–3907.
16. Larsson C, Emanuelsson L. Bone response to surface modified titanium implants – studies on the tissue response after 1 year to machined and electropolished implants with different oxide thickness. J Mater Sci Mater Med. 1997;8:721–729.
17. Park KH. Osseointegration of anodized titanium implants (thesis). Seoul Korea: Seoul National Univ.; 2003.
18. Sul YT, Johansson CB, Petronis S, Krozer A, Jeong Y, Wennerberg A, Albrektsson T. Characteristics of the surface oxides on turned and electrochemically oxidized pure titanium implants up to dielectric breakdown: the oxide thickness, micropore configurations, surface roughness, crystal structure and chemical composition. Biomaterials 2002;23:491–501.
19. Sul YT, Johansson CB, Jeong Y, Röser K, Wennerberg A, Albrektsson T. Oxidized implants and their influence on the bone response. J Mater Sci Mater Med. 2001;12:1025–1031.
20. Thomsen P, Larsson C, Ericson L, Sennerby L, Lausmaa J, Kasemo B. Structure of the interface between rabbit cortical bone and implants of gold, zirconium and titanium. J Mater Sci Mater Med. 1997;8:653–665.
21. Wennerberg A. The importance of surface roughness for implant incorporation. Int J Mach Tools Manufact. 1998;38:657–662.
22. Stenport VF, Johansson C, Heo SJ, Aspenberg P. Titanium implants and BMP-7 in bone: an experimental model in the rabbit. J Mater Sci Mater Med. 2003;14:247–254.
23. Sul YT, Johansson C, Wennerberg A, Cho LR, Chang BS, Albrektsson T. Optimum surface properties of oxidized implants for reinforcement of osseointegration: surface chemistry, oxide thickness, porosity, roughness, and crystal structure. Int J Oral Maxillofac Implants 2005;20:349–359.
24. Chun HJ, Cheong SY, Han JH, Heo SJ, Chung JP, Rhyu IC. Evaluation of design parameters of osseointegrated dental implants using finite element analysis. J Oral Rehabil 2002;29:565–574.

Correspondence: S. K. Kim, Department of Prosthodontics and Dental Research Institute, College of Dentistry, Seoul National University, 28-1, Yeungun-Dong, Chongno-Gu, 110-749, Seoul, Korea.
E-mail: ksy0617@snu.ac.kr